The Completion of a Geosynchronous Earth Orbit Survey with the Eugene Stansbery-Meter Class Autonomous Telescope

Corbin Cruz[(1)], Brent Buckalew[(1)], Jessica Arnold[(1)], Alyssa Manis[(2)], and Heather Cowardin[(2)]

[(1)] Jacobs, NASA Orbital Debris Program Office, NASA Johnson Space Center, Mail Code XI5-9E, 2101 NASA Parkway, Houston, TX 77058, USA; corbin.l.cruz@nasa.gov; brent.a.buckalew@nasa.gov; jessica.a.arnold@nasa.gov

[(2)] NASA Orbital Debris Program Office, NASA Johnson Space Center, Mail Code XI5-9E, 2101 NASA Parkway, Houston, TX 77058, USA; alyssa.p.manis@nasa.gov; heather.m.cowardin@nasa.gov

Abstract

The Eugene Stansbery-Meter Class Autonomous Telescope (ES-MCAT) is the primary optical sensor used by the NASA Orbital Debris Program Office (ODPO) to statistically characterize the geosynchronous Earth orbit (GEO) debris environment and support future Orbital Debris Engineering Model (ORDEM) releases. The ES-MCAT completed its first optical survey of the GEO region from 2020 to 2022. The primary goal of this survey was to autonomously collect and process GEO data with calculated photometric and astrometric uncertainties. A pointing plan was developed to provide uniform sampling within the region of interest (ROI) while accounting for predicted downtime due to insufficient observing conditions. Detections are autonomously correlated to the Space Surveillance Network (SSN) catalog to determine if objects are correlated targets (CTs) or uncorrelated targets (UCTs), the latter of which are of interest for modeling the GEO orbital debris environment.

To assess the size detection sensitivity over time and monitor the general performance of the telescope's optics and software, the optical throughput of the system and limiting magnitudes are evaluated on a routine basis. While the ability to operate the telescope autonomously and remotely allowed for the GEO survey to continue throughout the COVID-19 pandemic, travel restrictions hampered routine cleaning of the optics during this time, and the primary mirror degraded enough to require recoating. The mirror was removed in 2022, concluding the first GEO survey. The primary mirror received a new coating designed to be more robust against the harsh environment surrounding the ES-MCAT's location on Ascension Island, based on experience gained during operations over the first GEO survey.

In early 2023, the recoated primary mirror was reinstalled, and the second GEO survey was initiated. The primary goal of the second GEO survey is to characterize the evolving GEO debris environment with updated optics, software, and pointing strategies while allowing for the inclusion of non-GEO regimes or those that are outside of the ROI. While the pointing method implemented in the first survey allowed for adequate coverage of the ROI over two years, it has been improved to include pointings that avoid the Moon's position and the galactic plane to reduce software processing time and maximize the detection capabilities of fainter objects. This method also accounts for the changing weather patterns throughout the year and reduces coverage gaps in the ROI. Given the success of the first two-year GEO survey using autonomous operations, the ODPO is actively collaborating with the United States Space Force (USSF) to make the ES-MCAT a contributing sensor to the SSN.

This paper presents results from the first GEO survey including magnitude distributions and orbital parameters for CTs and UCTs. Details are provided for the automated processing pipeline and the optical system throughput for the previous and current primary mirror coatings. In addition, an updated

strategy for the second GEO survey to optimize coverage over the ROI is discussed, as are preliminary results from the ongoing second survey.

1 Introduction

The Eugene Stansbery-Meter Class Autonomous Telescope (ES-MCAT) recently completed its first optical survey to characterize the geosynchronous Earth orbit (GEO) debris environment after reaching full operational capability (FOC) in September 2021 [1, 5]. The first GEO survey was conducted from 14 April 2020 to 22 February 2022 throughout the COVID-19 pandemic, despite travel restrictions in place that temporarily paused routine maintenance including regularly scheduled cleanings of the primary mirror. During the survey, several methods were developed to routinely characterize telescope optics and monitor its performance. While a planned pointing strategy was followed for most of the survey's duration, manual pointings were included at the end of the survey to fill gaps in observational coverage due to weather events, unplanned maintenance, *etc*. Based on lessons learned, the pointing strategy was updated for the second survey to better account for downtime.

After the first GEO survey and when the reflectivity of the primary mirror could no longer be restored from cleanings, the mirror was removed for recoating with an enhanced protected silver coating by. This new coating has an updated composition, in addition to an overcoat using a commercial-off-the-shelf hydrophobic polymer coating and can better withstand the harsh environmental conditions of a sea-level, tropical observatory. Once the mirror was reinstalled in January 2023, the system throughput was reanalyzed and characterized to understand ES-MCAT's new detection capabilities, and the second GEO survey commenced. The survey goals are to continue characterizing the evolving GEO environment, increase the number of detections over the previous survey (aided by a newly coated primary mirror and the ability to perform regular cleanings), and expand observational coverage to new regions of the orbital debris (OD) environment.

The methodology, strategy, and results for both the first completed GEO survey and ongoing second GEO survey follow.

2 Optical System Throughput

Before initiating the first GEO survey, the optical throughput of the system was calculated [2]. After identifying each component of the optical system, individual optical response data was obtained from the respective manufacturers, shown in Fig. 1, between 390 nm and 980 nm due to the wavelength restrictions of obtained data. These optical component responses include the charge coupled device (CCD) quantum efficiency (QE), the reflectance of the primary (before recoating) and secondary mirrors, and the transmittance of the field corrector and CCD window.

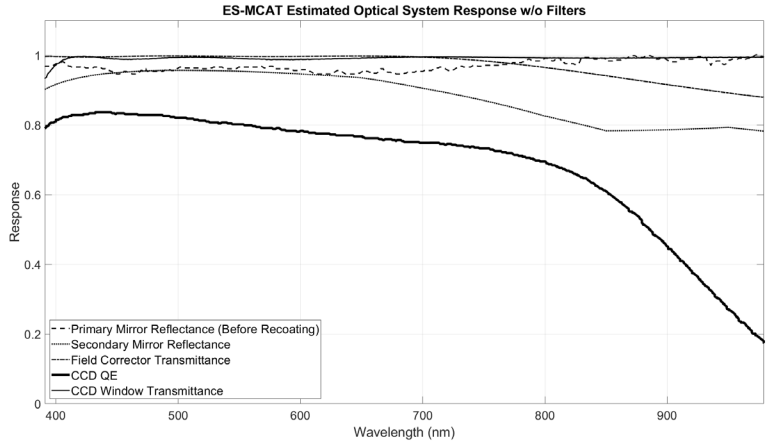

Fig. 1. Optical system response for all optical components installed in ES-MCAT within the wavelengths of 390 nm and 980 nm. Each contributes to the total throughput shown in Table 1.

A comparison of the primary mirrors' reflectance curves between the initial coating used in the first GEO survey (2020–2022) and the updated coating utilized during the second GEO survey (2023+) is shown in Fig. 2, with the curves labeled as ES-MCAT 1 and ES-MCAT 2, respectively. Upon inspection, they are very similar, with an average reflectance above 90% in both cases.

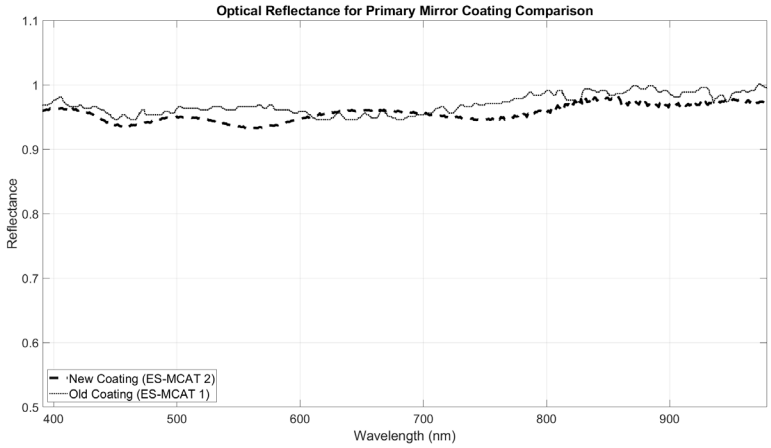

Fig. 2. Comparison of system response values between the previously coated primary mirror (ES-MCAT 1) and the newly coated primary mirror (ES-MCAT 2) within a range of wavelengths showing similar responses.

The individual components' optical response data were linearly interpolated between the installed filter wavelength regions of interest, including the Sloan Digital Sky Survey (SDSS) g'r'i'z' filters and the Johnson/Bessel-Cousins BVRI filters. These reflectance curves were multiplied with the averaged solar spectrum at sea-level. Finally, these products were integrated to give the total optical throughput in each installed filter bandpass for ES-MCAT with the previously installed primary mirror (ES-MCAT 1) and the newly coated primary mirror (ES-MCAT 2) (Table 1). A more detailed explanation of the throughput calculations is found in a previous characterization of ES-MCAT [2].

Table 1. Optical system throughput results for each installed optical filter

Filter	ES-MCAT 1 Flux (Arbitrary Units)	ES-MCAT 2 Flux (Arbitrary Units)
g'	118 ± 1.36	117 ± 1.34
r'	116 ± 1.35	115 ± 1.34
i'	82.8 ± 0.998	81.3 ± 0.982
z'	30.9 ± 0.560	30.4 ± 0.549
B	56.0 ± 1.04	58.29 ± 1.03
V	81.6 ± 1.23	79.9 ± 1.21
R	89.7 ± 1.22	89.3 ± 1.21
I	75.5 ± 0.855	74.0 ± 0.838

As shown in Table 1, the fluxes from the optical throughput analysis indicate that the SDSS g' and r' filters were ideal for observing OD with ES-MCAT during both the first and second GEO surveys. The flux values provided a basis for understanding the ideal optical characteristics of ES-MCAT and allowed for comparisons with upgrades or replacements of components in the system, such as the recoated primary mirror. A further study of solar analog stars suggested that the r' filter should be used in the first survey. In planning the second survey, the r' filter was again chosen to enable direct comparisons to the early part of the first GEO survey. The throughput flux results from the two different mirror coatings are within each other's uncertainties to within 3σ for each filter. This suggests that the performance for the optical system, with pristine components, would be similar.

3 Limiting Magnitude Evolution

In addition to the initial study of the optical system throughput, periodically analyzing the magnitudes from the dimmest detectable objects in a range of images and estimating a limiting magnitude from these values enabled continual checks of both the optics and software. Each night, a series of standard star field images was taken with sidereal tracking (ST) using the same filter as for GEO survey images taken the same night. The dimmest magnitudes from each ST image, found by the observatory control system (OCS) using isophotal photometry with a minimum signal-to-noise ratio of six, are plotted in Fig. 3 along with the measured primary mirror reflectivity, acquired using a handheld scatterometer that utilizes a 670 nm laser.

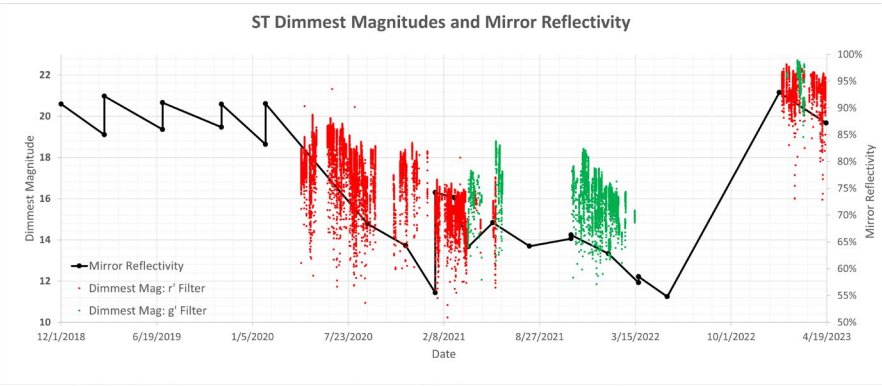

Fig. 3. Dimmest magnitudes and mirror reflectivity values plotted over time. Mirror reflectivity values are represented with a black dot and line, with the y-axis label on the right-hand side of the plot. The dimmest g' and r' filter magnitudes for each image are represented by green and red dots, respectively, with the y-axis label on the left-hand side of the plot.

The primary mirror reflectance curve shows natural degradation of the mirror reflectivity over time due to environmental effects (build-up of dirt, dust, and salt deposits from the humid salt air), the improvements gained with routine cleanings (approximately every 3 months from December 2018 to February 2020), and the effects of lapses in those cleanings (from March 2020 to January 2021, due to COVID-19 travel restrictions). The absence of dimmest magnitude datapoints between a range of dates in 2020 and 2021 was caused by miscellaneous unplanned maintenance. Periodic limiting magnitudes were estimated with these datapoints by selecting the most recent observational data spanning approximately two weeks and taking the median of the dimmest magnitudes over that time [3, 6]. At the onset of the first GEO survey, with the use of an SDSS r' filter and an exposure duration of 10 seconds, ES-MCAT's limiting magnitude was estimated as 19.48 ± 0.18. This magnitude represents objects approximately 10 centimeters in size when converted using the NASA Optical Size Estimation Model (OSEM) [4]. These estimates were vital in monitoring the system and making adjustments remotely. For example, as the primary mirror coating degraded non-uniformly throughout the optical spectrum, the SDSS g' filter was used in early 2021, which initially improved the limiting magnitude of the system by roughly one magnitude.

The new limiting magnitude of the system was established using data collected between January 2023 and February 2023. With 10-second exposures and use of the SDSS r' filter, similar to the beginning of the first GEO survey, the new limiting magnitude is approximately 22.28 ± 0.14. This limiting magnitude, when converted using the OSEM, is approximately 3 centimeters. The limiting magnitude/size and recoated primary mirror reflectivity (92.9% as compared to the previous maximum of 90.7%) indicate substantial improvements to both the optics and software detection capabilities.

The limiting magnitude during the first GEO survey was calculated when the primary mirror was already partially degraded, and its increased scatter likely caused this magnitude to become brighter than that of its pristine state. The limiting magnitude from the second GEO survey was calculated immediately after the reinstallation of the newly coated mirror, and it better represents the limiting magnitude of the optical system with pristine components.

4 Data Processing

Throughout the first GEO survey, updates to OCS were made to improve operations or image processing. Once the survey was completed, a single version of OCS was used to process the entire dataset. This step ensured result conformity for use in later modeling endeavors. The most important parameter is the minimum SNR of 6.0. Any object below this threshold would not be detected by OCS in the output sent to the orbital debris processing (ODP) correlation software. This was determined after thorough verification using previous telescopic data to maximize the detection of real objects and reduce false positives. After the survey data was processed with OCS, ODP then correlated the detected objects with the SSN catalog available from Space-Track.org and assigned each object as a correlated target (CT), which includes both intact objects and large OD, or an uncorrelated target (UCT).

Due to the degradation of optical throughput discussed previously, an object or point source that the automated software could detect at one point in time may not be detectable later. In addition to the optical throughput and limiting magnitude studies, OCS performance was investigated by inserting artificial resident space objects into images in a Monte Carlo manner and assessing how effective OCS was at finding those objects. Histograms of OCS detection completeness as a function of magnitude were created and analyzed to provide a datapoint to inform ORDEM of the system's capabilities at different points in time and improve the data quality of both GEO surveys. The data collected for the second GEO survey utilizes the same methods used during the first survey for calibrations and processing. The most recent, validated version of OCS and ODP are used on a computer cluster at the

NASA Johnson Space Center to reduce processing times from days to hours. Details on the Monte Carlo simulations are available in [5].

5 Pointing Strategy and Coverage

Like the first survey, the second GEO survey goal is to optimize sampling of GEO objects within a region of interest (ROI) with an expected value (EVAL) of 0.3 or greater. The EVAL gives the probability of detecting an object in a specific orbit while at a given field of view and time. This ROI is defined with inclination (INC) and right ascension of the ascending node (RAAN) in INC·cos(RAAN) and INC·sin(RAAN) space, centered at (7.5°, 0°) with a radius of 15° [6]. The ROI is shown in Fig. 4 along with the actual coverage of the first GEO survey with EVALs greater than 0.3 and greater than 0.2.

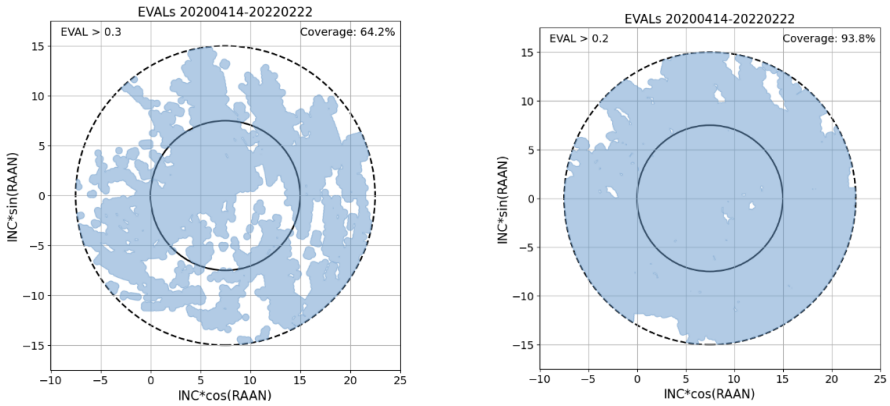

Fig. 4. (left) ROI coverage plot taken from the first GEO survey showing regions that exceeded an EVAL of 0.3. (right) ROI coverage plot taken from the first GEO survey showing regions that exceeded an EVAL of 0.2. Both plot titles are in the format YYYYMMDD.

A pointing strategy was developed for the first GEO survey to cover this ROI, as uniformly as possible, within the GEO debris belt over two years, while also allowing for certain lapses in coverage. Each night, a series of images were taken at two right ascensions (RA) and two declinations (Dec), with one set of RA and Dec during each half of the night. This was repeated for 24 more nights with decreasing Decs and increasing RAs, with the RAs trailing and leading the center of Earth's shadow by 15 degrees, and this 25-night pattern repeated for 350 nights. The resulting planned pointings are shown in Fig. 5, descriptively named the "Candy-Cane Method," along with the actual pointings from the first GEO survey.

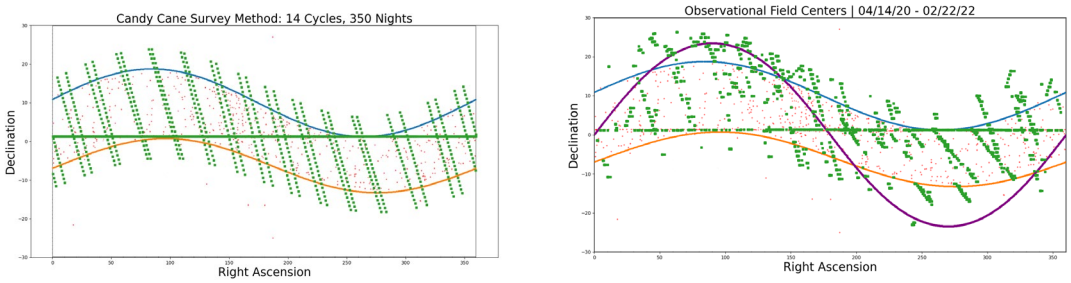

Fig. 5. (left) The pointing strategy implemented in the first GEO survey in RA/Dec space for 14 cycles, or 350 observational nights. Green squares represent planned field centers for each night, red markers represent catalogued GEO objects from January 2021, and the blue and orange curve represent the approximate upper and lower bounds of the GEO belt. (right) Actual field center pointings from the first GEO survey, with an additional purple curve representing the path of Earth's shadow.

Field center differences between the planned pointings and the actual pointings are attributed to weather downtime, unplanned maintenance, and Moon brightness preventing useful observations. These effects also impacted the overall coverage, shown in Fig. 4. The original survey method allowed for manual pointings, which enabled focused observations for reducing large coverage gaps in the ROI. While the basis of the pointing strategy from the first GEO survey remained the same for the second GEO survey, several updates were added to improve coverage in the ROI. First, the Moon illumination is avoided since images that are taken with the telescope pointing within about 20° of the Moon's position are either overexposed or make photometric calibrations impossible. Second, the galactic plane of the Milky Way is also avoided. Images taken within approximately 7.5° of the galactic plane contain large numbers of star trails making it difficult to detect objects and increasing processing time exponentially toward the plane center. Finally, the weather on Ascension Island tends to have a periodic trend, and the nightly observation availability is at its maximum in March and its minimum in September and October [7]. Field center coverage during the worse months, in terms of observation availability, are more spread out in December, shortening the cycle to 10 days, while those in months with clearer weather remain at 25 days. Cycles with 10 days have a better probability of repeating similar RAs than longer cycles; if a field center is missed during this time, it may better be covered in another cycle. The resulting planned field centers are illustrated in Fig. 6. Those field centers that do not seem to follow the planned pattern were modified to avoid either the Moon's position or that of the galactic plane.

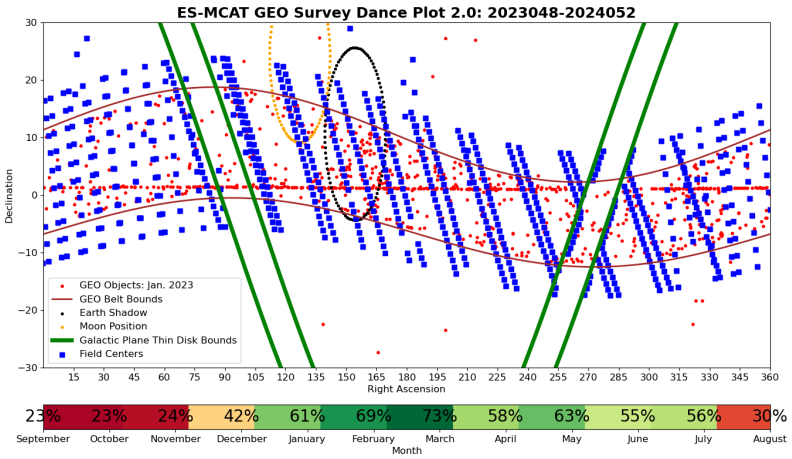

Fig. 6. Chart showing planned pointings/dance plot for the second GEO survey in RA/Dec space; blue squares represent the pointings for each night. Also plotted are the galactic plane thin disk bounds (green curves), cataloged GEO objects propagated to January 2023 (red dots), upper and lower bounds of the GEO belt (red curves), and nightly availability by month (color bar at bottom). Earth's shadow (±15 deg) and the Moon's position (±15 deg) for 21 February 2024 are also depicted by the black and yellow ellipses, respectively.

To understand how this updated pointing strategy affects the ROI, the field centers were processed through an in-house developed ODPO program, known as Tie-Dye, that simulates orbits with various INCs and RAANs based on the time of observation. This program was also utilized for previous telescopic measurements with the Michigan Orbital Debris Survey Telescope (MODEST) [8]. The predicted coverage is produced with EVALs indicated by a range of colors. This program was run for an ideal survey with no effects from weather along with an average survey with the nightly observation availability specified in Fig. 6. The effect is that certain regions of the Tie-Dye plot lose coverage, causing regions of the plot to show smaller total EVALs. These two weather scenarios are depicted in the ROIs in Fig. 7.

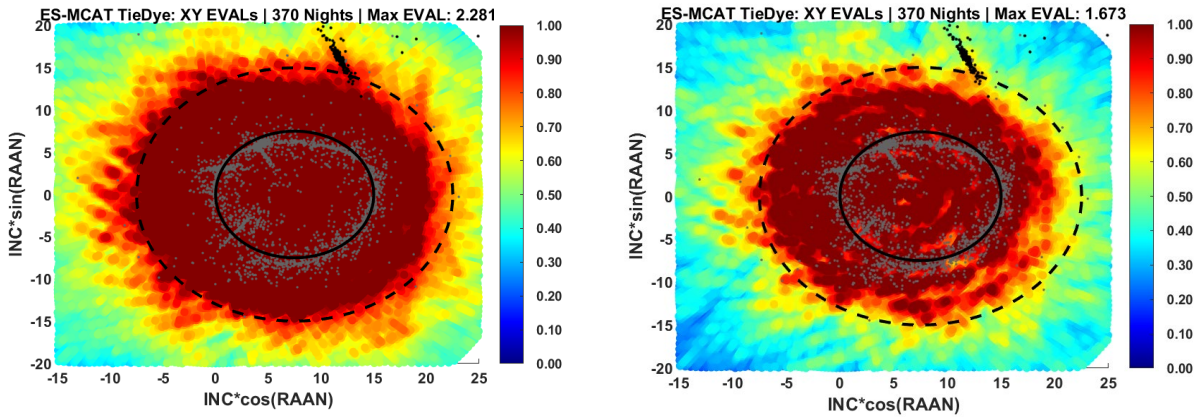

Fig. 7. ROI plots of coverage resulting from the pointing strategy of the second GEO survey in INC*cos(RAAN), INC*sin(RAAN) space. The ROI are indicated by the dashed black lines, modeled GEO debris (intacts and fragments propagated to late 2019) are shown with gray dots, and a modeled 2019 Titan Transtage breakup (propagated to December 2023) is shown with black dots. The EVALs within the plots are shown by a range of colors, indicated on the color bar on the right-hand side of each plot. The plot on the left utilized an ideal survey with no weather events, while the plot on the right removed certain field centers based on monthly availability (see Fig. 6).

Despite lower EVALs due to predicted weather events in the right-hand chart of Fig. 7, the minimum EVAL within the ROI is still at least 0.3, which meets the goal of the GEO survey. A Titan Transtage breakup that occurred in 2019 (International Designator 1976-023F, U.S. Satellite Catalog Number 8751), modeled with the NASA Standard Satellite Breakup Model (SSBM) and propagated to December 2023, is depicted in the charts with black dots. Also plotted are the modeled GEO debris objects from ORDEM 3.1 that are propagated to the end of 2019, marked with gray dots. The Titan 2019 breakup is part of the updated strategy that will include focused observations outside the ROI to ensure coverage of specific debris populations.

6 Survey Results

After processing the observational data from the first and ongoing second GEO survey through both OCS and ODP, the resulting detected objects were studied.

Of the total 921 objects observed during the first GEO survey, 83 objects were categorized as UCTs, and 838 were categorized as CTs. During the first three months of the second GEO survey, 320 objects were detected with 223 categorized as CTs and 97 as UCTs, surpassing those detected in the first GEO survey. This is likely owed to the newly recoated mirror and better detection capabilities of the system. The detections from the first and second surveys, along with the modeled GEO objects and Titan 2019 breakup, are also presented in the ROI plots in Fig. 8.

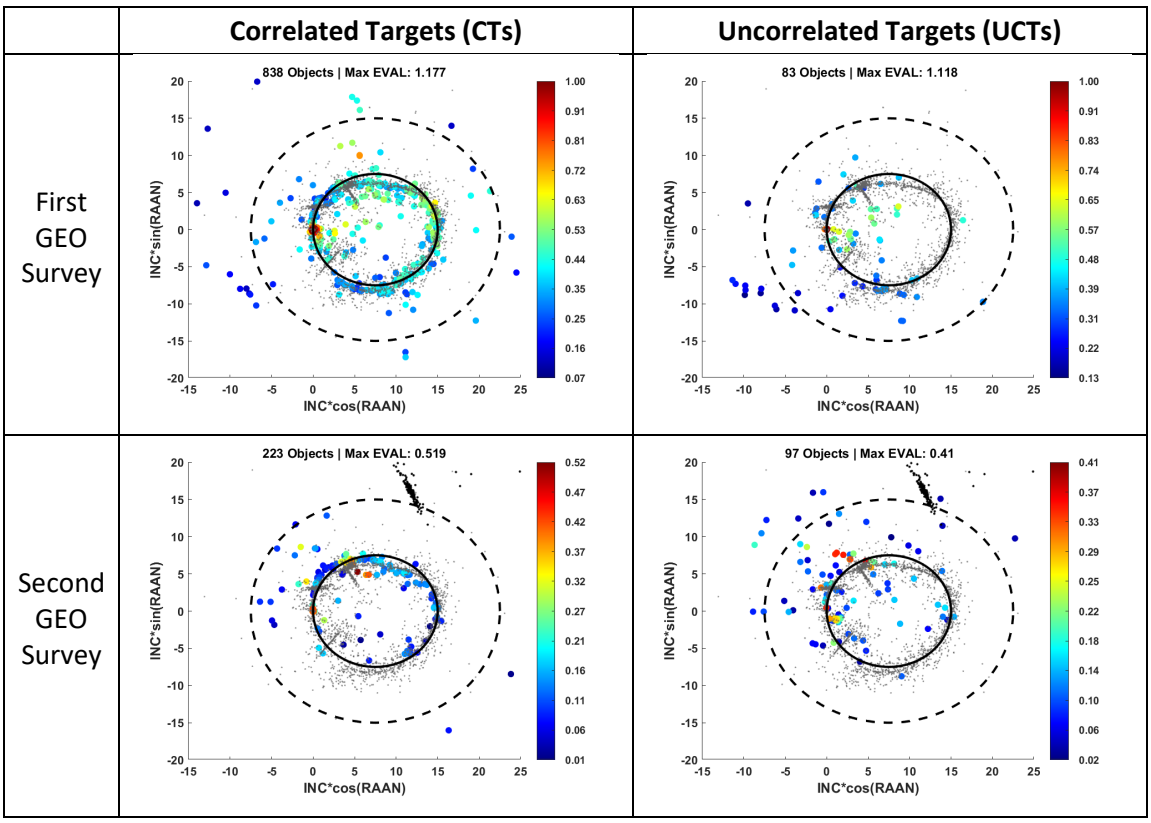

Fig. 8. ROI plots of detections from the first and second GEO surveys in INC*cos(RAAN), INC*sin(RAAN) space, similar to those in Fig. 7.

To further characterize the detected objects in the two surveys, the absolute magnitudes of each object were calculated from the measured apparent magnitudes and calibrated to GEO altitudes and plotted in histograms, shown in Fig. 9.

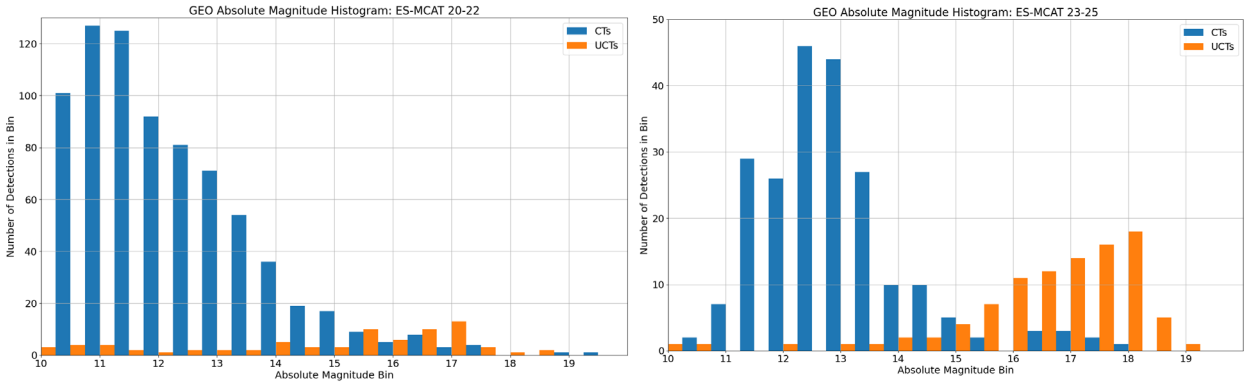

Fig. 9. Histograms of detected objects (CTs and UCTs), binned by absolute magnitude, for the first GEO survey (left) and the ongoing second GEO survey (right).
Note the different y-axis ranges between the plots.

By comparing the two histograms, the trend between the detection capabilities of the optical system and the type of object detected become apparent. With a dimmer limiting magnitude, more UCTs,

which have smaller sizes and thus dimmer magnitudes, are more easily detected. In particular, the number of detections increases up to approximately 18th magnitude, as opposed to the drop-off after approximately 17th magnitude seen in the first GEO survey. This roll-off is due to limitations of detection capabilities of the system, as the GEO debris population is expected to continue to increase at dimmer magnitudes or smaller sizes. This reinforces the importance of the earlier mentioned Monte Carlo simulations being conducted to better assess the capabilities of ES-MCAT at any point in time.

7 Summary

The strategy, autonomous processing methodology, and results from the first GEO survey completed by ES-MCAT were presented along with those from the ongoing second GEO survey. The impacts of COVID-19 and resulting travel restrictions were demonstrated by the effects of the degrading primary mirror coating on the limiting magnitude and detection capabilities of the system. With a recoated primary mirror, the detection capabilities during the second GEO survey surpass those at the beginning of the first survey, indicated by the increased number of dimmer detections and a higher limiting magnitude. Lessons learned during the first GEO survey enabled improvements to the pointing strategy, which better compensates for weather events and unplanned maintenance and reduces processing time. The second survey will also allow for pointings outside of the traditional ROI to cover possible new breakups, such as the 2019 Titan Transtage breakup. The ODPO is also working with the U.S. Space Force to make ES-MCAT, with its new capabilities, a contributing sensor to the SSN.

8 References

1. Lederer, S.M., *et al*. “NASA’s Orbital Debris Optical Program: ES-MCAT Nearing Full Operational Capability (FOC),” AMOS Technical Conference Proceedings, 2020.
2. Cruz, C.L., *et al*. “Characterization of the Eugene Stansbery-Meter Class Autonomous Telescope on Ascension Island,” AMOS Technical Conference Proceedings, 2021.
3. Hickson, P. “OCS: A Flexible Observatory Control System for Robotic Telescopes with Application to Detection and Characterization of Orbital Debris,” First International Orbital Debris Conference, Sugar Land, Texas, 2019.
4. Barker, E.S., *et al*. “Analysis of Working Assumptions in the Determination of Populations and Size Distributions of Orbital Debris from Optical Measurements,” Proceedings of the 2004 AMOS Technical Conference, Wailea, Maui, HI, pp. 225-235, 2004.
5. Hickson, P., *et. al*. “Automated Detection and Analysis of Resident Space Objects with the 1.3-Meter Eugene Stansbery-Meter Class Autonomous Telescope,” to be presented at the Second International Orbital Debris Conference, Sugar Land, Texas, 2023.
6. Cruz, C. *et al*. "Updates of the Eugene Stansbery-Meter Class Autonomous Telescope for Geosynchronous Orbit Survey Operations," Orbital Debris Quarterly News, Vol. 27, Issue 1, pp. 4-5, March 2023.
7. Lederer, S.M., *et. al*. “NASA’s Orbital Debris JAO/ES-MCAT Optical Telescope Facility on Ascension Island,” First International Orbital Debris Conference, Sugar Land, Texas, 2019.
8. Abercromby, K., *et al*. “A Summary of Five Years of Michigan Orbital Debris Survey Telescope (MODEST) Data,” IAC 2008.